PHYSICAL REVIEW C **77**, 064601 (2008)

Near threshold (γ, π^0) reactions for ^{4}He and ^{12}C

M. G. Barnett, R. Igarashi, R. E. Pywell,* and J. C. Bergstrom
Department of Physics and Engineering Physics, University of Saskatchewan
(Received 3 March 2008; published 4 June 2008)

The total cross section and angular distributions for the reaction $^4\text{He}(\gamma, \pi^0)$ from a cryogenic liquid helium target have been measured within 25 MeV of threshold using tagged photons and a large acceptance π^0 spectrometer at the Saskatchewan Accelerator Laboratory. The reduced isovector amplitude $p_3^{(+)}$ has been determined from the total cross-section measurement using a distorted-wave impulse approximation analysis. Refinements from earlier analytical methods, specifically an improved background event rejection scheme and a corrective tagged photon energy calibration analysis, have also yielded an improved estimate on the $p_3^{(+)}$ amplitude for the $^{12}\text{C}(\gamma, \pi^0)$ reaction explored previously.

DOI: 10.1103/PhysRevC.77.064601 PACS number(s): 25.20.Lj, 13.60.Le, 27.20.+n

I. INTRODUCTION

The study of π^0 photoproduction cross sections near threshold offers a unique opportunity to study nucleon structure and dynamics. This is possible by exploiting the chiral symmetry of quantum chromodynamics (QCD) and its spontaneous and explicit breaking in the low-energy regime. This method has been exploited by Bernard, Kaiser, Meißner and others [1–3] using heavy baryon chiral perturbation theory (CHPT) calculation to extract the so-called low-energy constants (LEC) that govern the cross sections at energies near threshold. Much experimental work has been done recently at Mainz and at the Saskatchewan Accelerator Laboratory (SAL) particularly on the proton [4–7].

When the formalism describing the cross sections is applied to a spin-zero nucleus, the elementary (γ, π^0) operator assumes a particularly simple form and offers the opportunity to extract the *nuclear* photoproduction amplitudes from the data and to compare them with the corresponding free-nucleon values.

Earlier work on ^{12}C [8] found a close correlation between the nuclear amplitude $p_3^{(+)}$ (defined in Sec. II) and the free-nucleon amplitude. This quantity is dominated by contributions from the $\Delta(1232)$ resonance, and the tentative conclusion was that the medium-modifications of the Δ, as they pertain to this amplitude, are negligible near threshold. This work is aimed at throwing further light on the validity of that conclusion.

The total cross section and angular distributions for the pion photoproduction reaction $^4\text{He}(\gamma, \pi^0)$ from a cryogenic liquid helium target have been measured within 25 MeV of threshold using tagged photons and a large acceptance π^0 spectrometer at the Saskatchewan Accelerator Laboratory (SAL). Previous measurements on this reaction have been performed but only at energies above 200 MeV [9,10]. The total cross section σ_T was directly measured using the π^0 spectrometer (Igloo) in its "closed" configuration; this setup offers the maximum pion acceptance of about 83% of 4π near threshold. The angular distribution was measured with Igloo in its open configuration; this offers the maximum pion angular resolution at the expense of a pion acceptance of just 28% of 4π near threshold. The same experimental setup was used for both the ^{4}He measurements reported here and the ^{12}C measurements reported previously, as both were studied concurrently. The new analytical methods developed here for the analysis of the ^{4}He data have also been applied to the ^{12}C data reported previously [8], and refined estimates for the parameters of that analysis are reported.

II. FORMALISM

The formalism required to describe π^0 photoproduction from ^{4}He is very similar to that previously described for ^{12}C [8], another spin-0 nucleus, and so only the most significant points will be discussed here.

The elementary transition matrix for photoproduction from a nucleon near threshold may be written generally as [1]:

$$\frac{M}{4\pi W} T \cdot \epsilon = i\vec{\sigma} \cdot \vec{\epsilon}(E_{0^+} + \hat{k} \cdot \hat{q} P_1) + i(\vec{\sigma} \cdot \hat{k})(\vec{\epsilon} \cdot \hat{q}) P_2 + (\hat{q} \times \hat{k} \cdot \vec{\epsilon}) P_3, \quad (1)$$

where M is the nucleon mass, W is the πN invariant mass, and $\vec{q}$ and $\vec{k}$ are the pion and photon momenta in the πN center-of-mass frame. E_{0^+} describes the S-wave production of pions and is a complex quantity even at relatively low energies. The amplitudes $P_{1,2,3}$ are associated with P-wave pion production and may be considered as real quantities at low energy; these amplitudes are defined in terms of the fundamental P-wave amplitudes as follows:

$$\begin{aligned} P_1 &= 3E_{1^+} + M_{1^+} - M_{1^-} \\ P_2 &= 3E_{1^+} - M_{1^+} + M_{1^-} \\ P_3 &= 2M_{1^+} + M_{1^-}, \end{aligned} \quad (2)$$

where E_{1^+} is an electric quadrupole amplitude and M_{1^+} and M_{1^-} are magnetic dipole amplitudes corresponding to total πN angular momenta $j = 3/2$ and $1/2$, respectively.

When applied to elastic transitions for a self-conjugate, spin-zero nuclear system with the impulse approximation invoked, all terms in Eq. (1) vanish from angular-momentum

*Corresponding Author: rob.pywell@usask.ca

considerations except for the final term, proportional to P_3. Further, because helium is an isoscalar nucleus, π^0 production is sensitive to only the isovector-even part of P_3, denoted as $P_3^{(+)}$ and defined in terms of the proton and neutron amplitudes by:

$$P_3^{(+)} = \frac{1}{2}[P_3(p) + P_3(n)]. \tag{3}$$

At low energy, the P-wave multipole amplitudes are conjectured to be simply proportional to kq in the πN frame [11], so that $P_3^{(+)}$ can be written as:

$$P_3^{(+)} = p_3^{(+)} \cdot kq, \tag{4}$$

where the reduced amplitude $p_3^{(+)}$ is presumed to be constant.

Using the ansatz of Eq. (4), the elastic nuclear differential cross section in the plane-wave impulse approximation (PWIA) reduces to:

$$\frac{d\sigma}{d\Omega} = \frac{A^2}{2}\left(\frac{q}{k}\right)\left[p_3^{(+)} \cdot kq\right]^2 F^2(Q)\sin^2\theta_\pi, \tag{5}$$

where k and q are evaluated in the πA frame and $F(Q)$ is the matter distribution form factor and the momentum transfer is defined by $\vec{Q} = \vec{k} - \vec{q}$. Note that $p_3^{(+)}$ enters as a scale factor and remains so in the more accurate distorted-wave impulse approximation (DWIA) treatment of the cross sections.

The form used for $F(Q)$ was an extension of the form factor used in Ref. [12]:

$$F(q) = (1 - (a^2q^2)^6)\mathrm{e}^{-b^2q^2}, \tag{6}$$

where a and b are phenomenological parameters. To account for high-q behavior, a is fixed to 0.316 fm and b is fixed to 0.675 fm.

The DWIA model differs from the PWIA model by an energy-dependent scale factor R [13]. A further refinement to this scale factor is given by Ref. [14], which renormalizes R by a factor of 0.988. In the energy range of interest, R boosts the form factor by 16–24%, depending on the photon energy. Although the pion wave distortions described by the DWIA model are more complex for angular distributions due to interference between competing partial waves altering the angular dependence, this effect is minimal at low energies [13]. To a good approximation, then, the factor R enters the cross section as an overall scale factor with no angular dependence, greatly simplifying this analysis.

Although $p_3^{(+)}$ is presumed to be energy independent, there is, as reported in Ref. [8], some theoretical evidence for a weak energy dependence near threshold. This will be accommodated using a phenomenological adjustment factor α [8]:

$$p_3^{(+)} \to p_3^{(+)}[1 + \alpha(E - E_{\mathrm{th}})], \tag{7}$$

where E_{th} is the production threshold energy and α is a constant whose value is to be determined. Hence, a two parameter fit will be applied to the total cross-section measurement to determine the values of $p_3^{(+)}$ and α.

III. EXPERIMENTAL DETAILS AND RESULTS

This experiment was performed at the Saskatchewan Accelerator Laboratory (SAL) using the tagged photon facility [15], the π^0 spectrometer "Igloo" [16], and techniques similar to those employed for previously reported measurements [4,5,8]. Bremsstrahlung was generated by a 205.9-MeV electron beam with an energy spread of about 50 keV and a duty factor of 60–70%, as provided by the pulse-stretcher ring EROS. The photon tagger was equipped with a 62-channel medium-resolution detector array that permitted a survey over an excitation range of 25 MeV using a single setting of the tagging spectrometer. Each channel of the array spanned about 500 keV in tagged photon energy.

The π^0 spectrometer Igloo, described in detail in Ref. [16], consists of a rectangular box of 68 lead glass detectors symmetrically arranged to define a hollow cave of dimensions $100 \times 40 \times 40$ cm. In this "closed" configuration, Igloo is employed exclusively for total cross-section measurements, exploiting its large geometric acceptance of 83% of 4π near threshold. For measurements of pion angular distributions, Igloo is split along a diagonal of the cave, and each L-shaped arm is retracted 42 cm to enhance the angular resolution of π^0-decay photons. In this "open" mode, pion acceptance is reduced to 28% of 4π near threshold. Pion emission angles are reconstructed from the respective decay photon angles and energies using the reconstruction algorithm described in Ref. [16]. The helium target was a cryogenic liquid target with a thickness of 1.51 g/cm^2. The target was contained within a mylar cell located at the geometric center of Igloo.

The analysis reported here uses an improved method for modeling the background in the total neutral pion yield required to extract the total cross section as a function of energy. Events observed below threshold are known to be due to background. In the previously reported analysis of the ^{12}C data [8] it was assumed that the background contribution was constant with energy, a reasonable assuption over the small energy range. However, a more detailed analysis has revealed that there is an energy dependence to the acceptance of such background through the analysis cuts. This energy dependence has been mapped out by analyzing known background events from below threshold as if they were at higher energies. This improved background model has been used for both the ^{4}He and ^{12}C results reported here.

The photon energy calibration is of vital importance to the analysis. The photon energy is found from the photon tagging technique as reported in Ref. [15]. However shifts in the energy represented by a particular tagger channel can be caused by two factors: a change in beam energy and changes in the magnetic field within the tagging spectrometer. It is therefore possible that there is a change in the nominal energy for a particular beam setup. The π^0 photoproduction threshold is a well-understood quantity and was used to determine the energy calibration shift for a particular data run. This energy calibration is performed simultaneously with the parameter fitting and therefore the method is described in Sec. IV. The energy calibration shifts determined are listed in Table I. Note that there are only slight differences between runs, suggesting that the experimental apparatus was relatively stable over

TABLE I. Energy calibration shifts.

Total cross-section run	Angular cross-section run	Energy shift (MeV)
#1	#1	-0.84 ± 0.05
#2	#2	-0.90 ± 0.02
#3	#3	-0.98 ± 0.04
#4	–	-0.90 ± 0.06

the time of the experiment. The energy calibrations for the first three total cross-section measurements apply also to the three angular-distribution measurements as total cross-section and angular-distribution measurements were always in interleaved run segments. Note that only three angular-distribution measurements were performed—the fourth total cross-section measurement has no angular-distribution counterpart.

The total cross section within 25 MeV of threshold ($E_{\rm th} = 137.4$ MeV) is shown in Fig. 1. Four separate trials were performed using the helium target; the graph shows the cross section for each trial with the energy calibration shifts applied. Note the excellent consistency between the four trials. The systematic uncertainty in the total cross section includes a contribution from the target thickness measurement but is dominated by our understanding of the detector efficiency of the spectrometer in the "closed" configuration [8]. The total systematic uncertainty is estimated to be 2%.

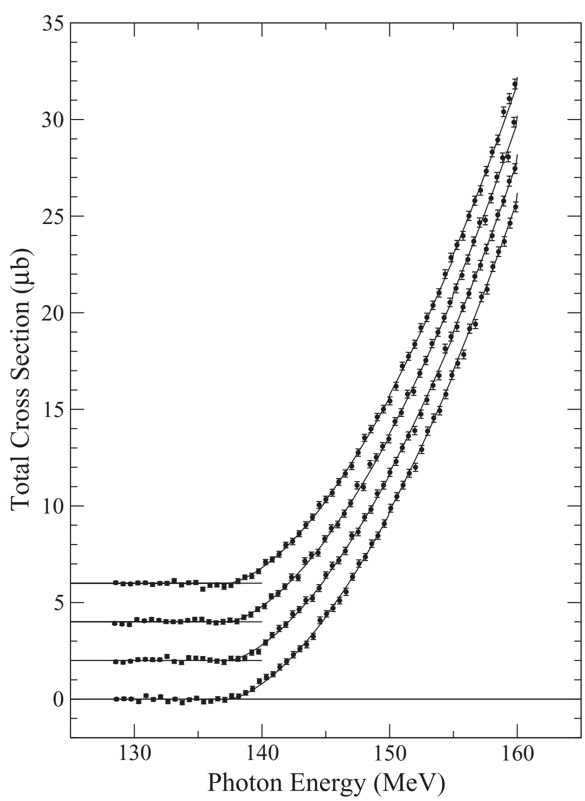

FIG. 1. The total π^0 production cross section as a function of photon energy for ^{4}He. The solid circles are the data and the solid line is the theoretical fit. For clarity the four data runs are shown offset verticalliy from each other by 2 μb.

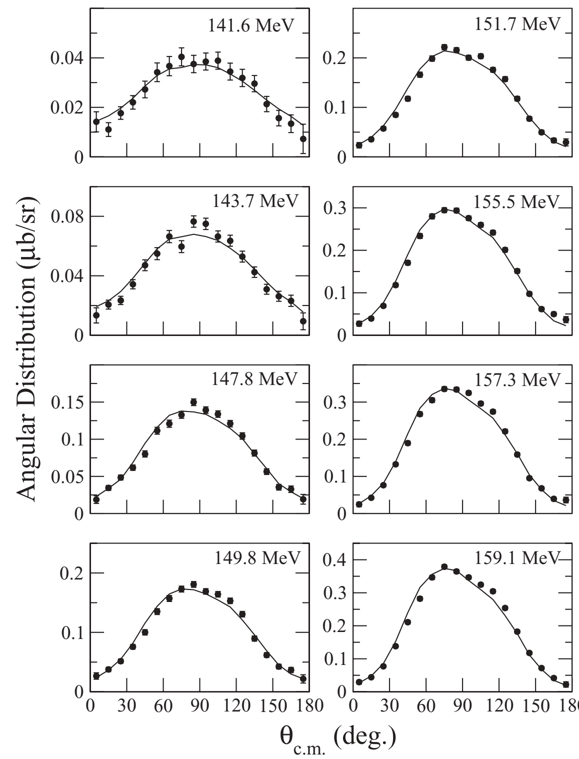

FIG. 2. Some examples of the ^{4}He(γ, π^0) angular distributions. Each point subtends about 2 MeV of excitation and 10° of angle. These are not physical cross sections but rather represent the cross section folded with the angular response of the π^0 spectrometer. The solid curves represent the fit to data as described in the text.

The angular distributions are presented in Fig. 2, using angular bins 10° wide. Each distribution collects the data from four consecutive tagger channels and thus subtends about 2 MeV of excitation. Further, the data from three distinct data runs have been combined; the effect of this merge on the energy calibration process will be discussed in Sec. IV. Note that the angular distributions shown do not reflect the true pion angular distributions; rather, they represent the pion angular distributions folded with the finite angular resolution of the π^0 spectrometer, typically 25°–35° FWHM. This accounts for the excess yield at the extreme forward and backward angles where the physical cross sections eventually vanish as in Eq. (5).

IV. ANALYSIS OF THE CROSS SECTIONS

The objective of this analysis is to determine the reduced isovector amplitude $p_3^{(+)}$ and its possible near-threshold energy dependence in the form of the first-order correction factor α for a ^{4}He nuclear-scattering target. Both parameters, as well as the calibration for the energy spectrum of the tagger for each experimental run are calculated from the total cross section. The angular distributions serve as tests of the model's description of angular dependence but are not used in the determination of any parameter values.

The first parameters to be determined are the energy calibration shifts, which may result from slightly different accelerator setup conditions and photon tagger magnetic field variations that may occur between one run and another. These energy shifts are determined using a reduced subset of the total cross-section data. To emphasize the importance of the production threshold energy as the calibration point and to remove the unwanted additional flexibility that the correction factor α provides at higher energies, the fit to determine the calibration shifts uses only those data points below a selected cutoff energy. In this energy range, $p_3^{(+)}$ is assumed constant with $\alpha = 0$; thus, the fit is over five parameters: the energy calibration shifts for the four data sets and a temporary value for $p_3^{(+)}$. The cutoff energy has to be chosen carefully: if it is too close to threshold, few data points would remain and the data will not have sufficient statistical accuracy to constrain the fit, and if it is too far above threshold, the assumption that $p_3^{(+)}$ is constant (that is, $\alpha = 0$) will no longer be valid. The cutoff energy of 7.0 MeV above threshold was employed as it is the cutoff energy that yielded the lowest χ^2 value in the subsequent fit to find $p_3^{(+)}$ and α and using the energy calibration determined by the low-energy $\alpha = 0$ fit. Thus an iterative process was used to determine the energy calibrations parameters along with $p_3^{(+)}$ and α.

Given the energy calibration shifts in Table I, the data were reanalyzed to determine $p_3^{(+)}$ and α using the complete energy range out to 25 MeV above threshold. The results of the two parameter fit are:

$$\begin{aligned} p_3^{(+)} &= (10.82 \pm 0.10) \times 10^{-3}/m_\pi \\ \alpha &= (3.44 \pm 0.45) \times 10^{-3}/\text{MeV}. \end{aligned} \tag{8}$$

The resulting fit has a reduced-χ^2 of 0.87 and is shown by the solid line in Fig. 1. Note the excellent fit obtained for all four data runs.

The angular distributions at varying photon energies were fitted to the DWIA model using the overall normalization as the single fit parameter. Because $p_3^{(+)}$ is constant at a particular energy and enters the theoretical cross section as an overall scaling factor only, it is absorbed into the overall normalization and hence is not used in the fit for the angular distributions. The normalization parameter also includes contributions from the low geometric efficiency of the π^0 spectrometer in its open configuration. To perform all angular fits as a set, the three experimental runs are merged together according to tagger channel bins, and an energy calibration of -0.91 MeV, the mean of the individual data run calibrations, is applied to the merged data set. Because the difference between each data run's energy shift and the mean energy shift (at most 0.07 MeV) is much smaller than the width of each bin (about 2 MeV), this process does not add significantly to the errors in the final result. The fits for several energies are shown in Fig. 2. The general characteristics of the angular distributions are well reproduced by the DWIA model and the detector simulation.

The analysis refinements to the background subtraction procedure, and to the method of determining the energy calibration, have been applied to a reanalysis of the π^0 production cross section near threshold for ^{12}C first described in Ref. [8]. The previous values for $p_3^{(+)}$ and α using a flat background subtraction and with only a basic estimate of the energy calibration shifts were:

$$\begin{aligned} p_3^{(+)} &= (11.24 \pm 0.15) \times 10^{-3}/m_\pi \\ \alpha &= (1.20 \pm 0.36) \times 10^{-3}/\text{MeV}. \end{aligned} \tag{9}$$

When the new fitting algorithm was applied to determine the energy calibration shift, a value of 0.00 MeV was expected if the prior results were in fact calculated with the optimal energy calibration. Instead, an energy shift of $+0.22 \pm 0.17$ MeV was found, with a better reduced-χ^2. The result of this reanalysis, changing only the energy calibration, is

$$\begin{aligned} p_3^{(+)} &= (10.91 \pm 0.26) \times 10^{-3}/m_\pi \\ \alpha &= (2.4 \pm 1.0) \times 10^{-3}/\text{MeV}. \end{aligned} \tag{10}$$

The results now show a reduced $p_3^{(+)}$ and a slightly higher energy-dependence parameter α, although these values still agree within error to the results previously published.

The use of the more physically motivated background subtraction produces a more significant change in the results. A better reduced-χ^2 of 0.53 is found with an energy calibration shift of $+0.27$ MeV. The result show a further decreased $p_3^{(+)}$ and an increased α:

$$\begin{aligned} p_3^{(+)} &= (10.38 \pm 0.43) \times 10^{-3}/m_\pi \\ \alpha &= (2.8 \pm 1.7) \times 10^{-3}/\text{MeV} \end{aligned} \tag{11}$$

V. DISCUSSION AND CONCLUSION

We present new measurements of the total cross section and angular distributions of the ^{4}He(γ, π^0) reaction within 25 MeV of threshold.

The analysis of these measurements benefit from an improved background subtraction technique and an improved determination of the tagged photon energy calibration.

The total cross section is analyzed to determine the isovector amplitude $p_3^{(+)}$ and examine the possibility of a weak energy dependence in $p_3^{(+)}$ using the energy-slope parameter α. The results of this analysis yield for the ^{4}He(γ, π^0) reaction:

$$\begin{aligned} p_3^{(+)} &= (10.82 \pm 0.10) \times 10^{-3}/m_\pi \\ \alpha &= (3.44 \pm 0.45) \times 10^{-3}/\text{MeV}. \end{aligned}$$

By applying the new analytical techniques developed here to previous data for the ^{12}C(γ, π^0) reaction, the estimate for the reduced isovector amplitude for that reaction was refined to:

$$\begin{aligned} p_3^{(+)} &= (10.38 \pm 0.43) \times 10^{-3}/m_\pi \\ \alpha &= (2.77 \pm 1.70) \times 10^{-3}/\text{MeV}. \end{aligned}$$

The uncertainties in both of the above $p_3^{(+)}$ values reflect counting statistics, uncertainty in the measured photon tagging efficiencies, and background subtractions. The additional 2% systematic uncertainty is not included.

The value of $p_3^{(+)}$ determined for ^{4}He [Eq. (8)] appears to be comparable to that from a carbon target [Eq. (11)], although both are significantly lower than the $p_3^{(+)}$ amplitudes for a free nucleon predicted by chiral perturbation theory (CHPT) [2] or a formulation employing an effective Lagrangian with the Δ resonance as an explicit degree of freedom [2,17,18].

$$p_3^{(+)} = 11.4 \text{ CHPT prediction}$$
$$p_3^{(+)} = 12.4 \text{ effective Lagrangian}$$

Note that the amplitudes determined for ^{4}He and for ^{12}C are lower than either prediction, although they are significantly closer to the CHPT value.

The present results would suggest that there is some modification of $p_3^{(+)}$ in the nuclear medium from the free-nucleon value. The modification is approximately the same for ^{4}He and ^{12}C.

There may be a hint that the modification to $p_3^{(+)}$ is larger in nuclei with greater nucleon number because the value of $p_3^{(+)}$ is lower for ^{12}C than for ^{4}He, although this conclusion may not be justified by the errors in $p_3^{(+)}$ and further work would be needed to investigate this. Analysis of as yet unanalyzed data for ^{16}O taken at SAL would be useful in this regard.

ACKNOWLEDGMENT

The authors gratefully acknowledge the support for this work from the Natural Sciences and Engineering Research Council of Canada.

[1] V. Bernard, N. Kaiser, and U.-G. Meißner, Z. Phys. C **70**, 483 (1996).
[2] V. Bernard, N. Kaiser, and U.-G. Meißner, Phys. Lett. **B378**, 337 (1996).
[3] V. Bernard, N. Kaiser, and U.-G. Meißner, Eur. Phys. J. A **11**, 209 (2001).
[4] J. C. Bergstrom, J. M. Vogt, R. Igarashi, K. J. Keeter, E. L. Hallin, G. A. Retzlaff, D. M. Skopik, and E. C. Booth, Phys. Rev. C **53**, R1052 (1996).
[5] J. C. Bergstrom, R. Igarashi, and J. M. Vogt, Phys. Rev. C **55**, 2016 (1997).
[6] A. Schmidt, P. Achenbach, J. Ahrens, H. J. Arends, R. Beck, A. M. Bernstein, V. Hejny, M. Kotulla, B. Krusche, V. Kuhr *et al.*, Phys. Rev. Lett. **87**, 232501 (2001).
[7] M. Fuchs, J. Ahrens, G. Anton, R. Averbeck, R. Beck, A. M. Bernstein, A. R. Gabler, F. Härter, R. D. Harty, S. Hlavác *et al.*, Phys. Lett. **B368**, 20 (1996).
[8] J. C. Bergstrom, R. Igarashi, and J. M. Vogt, Phys. Rev. C **55**, 2923 (1997).
[9] F. Rambo, P. Achenbach, J. Ahrens, H. J. Arends, R. Beck, S. J. Hall, V. Hejny, P. Jennewein, S. S. Kamalov, M. Kotulla *et al.*, Nucl. Phys. **A660**, 69 (1999).
[10] D. R. Tieger, E. C. Booth, J. P. Miller, B. L. Roberts, J. Comuzzi, G. W. Dodson, S. Gilad, and R. P. Redwine, Phys. Rev. Lett. **53**, 755 (1984).
[11] E. Amaldi, S. Fubini, and G. Furlan, *Pion Electroproduction*, Springer Tracts in Modern Physics 83 (Springer-Verlag, Berlin, 1979), p. 147.
[12] C. R. Ottermann, G. Köbschall, K. Maurer, K. Röhrich, C. Schmitt, and V. H. Walther, Nucl. Phys. **A436**, 688 (1985).
[13] A. A. Chumbalov, R. A. Eramzhyan, and S. S. Kamalov, Z. Phys. A **328**, 195 (1987).
[14] S. Kamalov 1998 (private communication).
[15] J. M. Vogt, R. E. Pywell, D. M. Skopik, E. L. Hallin, J. C. Bergstrom, and H. S. Caplan, Nucl. Instrum. Methods A **324**, 198 (1993).
[16] J. M. Vogt, J. C. Bergstrom, R. Igarashi, and K. J. Keeter, Nucl. Instrum. Methods A **366**, 100 (1995).
[17] M. Benmerrouche, R. M. Davidson, and N. C. Mukhopadhyay, Phys. Rev. C **39**, 2339 (1989).
[18] R. M. Davidson, N. C. Mukhopadhyay, and R. S. Wittman, Phys. Rev. D **43**, 71 (1991).